

GAS PHASE RELATIVE PERMEABILITY CHARACTERIZATION ON TIGHT GAS SAMPLES

Y. Wang, Z. Chen, V. Morah, R. J. Knabe and M. Appel
Shell International E & P, Inc., Houston, USA

This paper was prepared for presentation at the International Symposium of the Society of Core Analysts held in Austin, Texas, USA 18-21 September, 2011

ABSTRACT

Relative permeability of the formation fluids is an essential input in reservoir characterization, dynamic modeling, and production prediction. In this work, a method combining evaporation and unsteady state pressure falloff technique is developed to measure gas phase relative permeability on tight gas cores for both drainage and imbibition cycles. Toluene is used to mimic formation water and its saturation is varied by evaporation and determined by mass balance. Nitrogen gas is used to imitate the hydrocarbon fluid, and the gas effective permeability at certain toluene saturations is measured by the pressure falloff technique.

The method greatly reduces the measurement duration, and provides a relatively simple and effective way to characterize the gas phase relative permeability for tight gas cores. It has been applied on ~30 tight gas cores from various fields. Results show that the gas relative permeabilities follow the Corey model with a Corey exponent of ~2 for drainage cycle and ~3 for imbibition cycle. The assumptions are studied by both numerical modelling and separate experiments.

INTRODUCTION

As production from tight gas formation grows, determination of relative permeability of the formation is becoming more and more important. It is an essential input in reservoir characterization, dynamic modeling, and production forecasting. Tight gas normally refers to low permeability reservoirs mainly producing dry natural gas. Nowadays, production from formation of microD or tighter increasingly contributes to the energy supply. Determination of microD or sub-microD permeability itself is challenging. For the case of relative permeability, the determination is further complicated by its dependence upon partial liquid saturation and confining stresses.

Due to the water-wet nature of the majority of tight gas reservoirs, gas phase relative permeability has been the first focus of study. Ref. [1] and [2] provided comprehensive literature overviews on gas relative permeability using different methods. Among those methods, traditional techniques of injecting gas and water under steady-state condition involve elaborated stress and flow control. Consequently, those techniques are often very time-consuming and associated with large uncertainties in flow rate measurements.

Several alternative methods have been applied to measure the relative permeability, including capillary pressure measurements on unconfined samples, centrifuge, and evaporation techniques. In an evaporation method, liquid saturation is varied through evaporation, and the effective permeability to gas is measured by either steady-state flow [3, 4] or unsteady state pressure transient experiments [5, 6]. Compared with the displacement type of experiment, it greatly reduces the time to reach certain fluid saturation, thus reducing the experiment turnaround time. In most evaporation type experiments, water/brine and nitrogen/air are used as wetting and nonwetting fluids, respectively.

In this work, we describe a relatively simple and effective method to measure the gas phase relative permeability on tight gas cores. In this method, toluene is used to mimic the formation water as toluene shows similar wettability to water. In addition, compared to water, toluene is easier to flow and to be injected. It also avoids potential salinity change during evaporation. Gas effective permeability at certain liquid saturation is measured by unsteady state pressure falloff method. Nitrogen is used to imitate the hydrocarbon gas. As the majority of tight gas reservoirs are water wet, water relative permeability is much smaller than that for gas over a wide range of water saturation. Therefore, for a range of water saturation, water can be assumed immobile during gas flow. We will introduce experiment setup and measurement procedures, present some of the measured results, discuss the uncertainties, and evaluate the assumptions through both experiments and simulations.

EXPERIMENT

USS Pressure Falloff Method

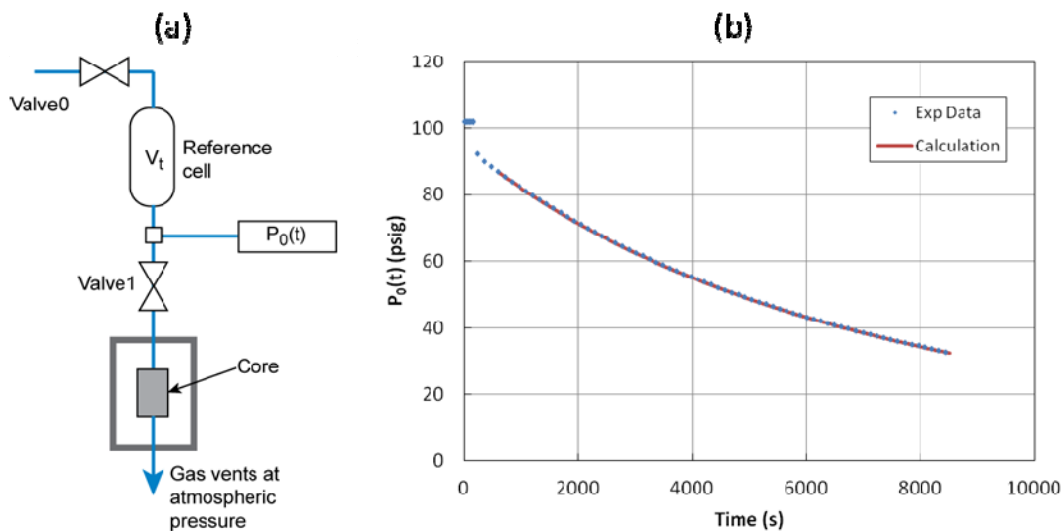


Figure 1: (a) Schematic of the unsteady state (USS) pressure falloff experiment. (b) Upstream pressure decay for O006 in a falloff measurement.

The unsteady state (USS) pressure falloff method was first developed by Jones [7], and has been applied in permeability measurements for tight cores [8]. In this paper, it is also called pressure falloff or falloff for simplicity. The experimental setup is shown schematically in Figure 1(a). It consists of a Hassler type core holder, a reference vessel, a pressure transducer, and several valves. The volume of the reference cells ranges from 10 cc to 150 cc to accommodate a range of core with different porosity and permeability. Proper selection of the reference vessel can reduce the measurement duration and optimize sensitivity. At the beginning of measurement, the core sample is under atmospheric pressure with its downstream side open to the air. The reference cell is pre-filled with nitrogen gas at ~100 psig. When the gas in the cell achieves thermal equilibrium and the pressure reading is stabilized, the Valve1 is opened, and the upstream pressure is recorded as nitrogen flows through the core sample. The setup for falloff method is relatively simple. In laboratory, one can easily have several core samples measured at the same time in multiple core holders and increase the sample throughput.

Figure 1(b) shows both the measured and calculated pressure decay as function of time, $P_0(t)$. The data analysis is largely based on the discussion by Jones [7]. For ideal gas flow in a 1D homogeneous porous medium with length L and cross sectional area A , under constant mass flow condition, $P_0(t)$ decays with time from Darcy's Law as:

$$-\frac{V_r}{P_0(t)} \frac{dP_0(t)}{dt} = i + mP_0(t), \quad (1)$$

Where $P_0(t)$ is the gauge pressure, V_r is the volume of reference cell, $m = k_{abs}A/(2\mu L)$, and $i = 2(P_a + b)m$. k_{abs} is the absolute Klinkenberg-corrected permeability, μ is the gas viscosity, P_a is the atmospheric pressure, and b is the gas slip factor. Eq. (1) shows that a plot of $-[V_r/P_0(t)][dP_0(t)/dt]$ vs. $P_0(t)$ is a straight line with the slope of m and intercept of i , from which both k_{abs} and b are obtained. For the data displayed in Figure 1(b), k_{abs} is 0.004 mD.

By measuring the pressure change directly instead of the flow rate, the falloff method is particularly useful in the low permeability measurement. Before being applied to the measurement of relative permeability, the falloff method has been calibrated by comparing Klinkenberg-corrected permeabilities derived from falloff, steady-state, and pore pressure oscillation methods (SPPOP) [9]. Figure 2 shows the comparison between falloff and SPPOP on a set of tight gas cores. The permeability from the falloff method agrees reasonably with that from the SPPOP. For $k < 0.001$ mD, pressure falloff is very slow and potentially sensitive to temperature change. Consequently, the uncertainties in measurement and data analysis are larger, compared to the SPPOP measurements. On the other hand, the gas slip factor is poorly determined from falloff method, possibly due to the low and narrow pore pressure range investigated and the missing back flow control.

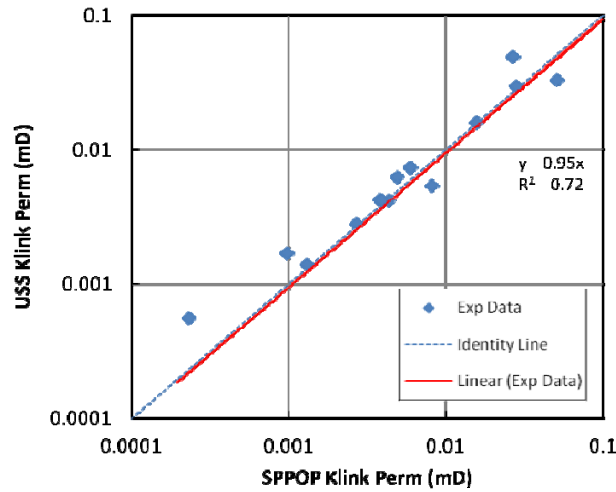


Figure 2: Comparison of Klinkenberg permeability from falloff method and pore pressure oscillation method (SPPOP).

Core Preparation and Measurement Procedure

The tight gas samples used in this work originated from Wyoming, USA and the North Sea. They were typically 1 inch in diameter and up to 1.5 inch long. Plugs were cleaned and oven dried at 60 °C. Before relative permeability measurements were conducted, the Klinkenberg permeability (k_{abs}) was measured on a dry clean core plug. For those plugs investigated, k_{abs} varied between 0.0006 mD and 0.3 mD. The core plug was subsequently saturated with toluene. To achieve 100% saturation in tight cores, the core sample was initially vacuum-saturated, followed by pressure saturation. After the core was fully saturated, its pore volume was determined from Archimedes principle using toluene. The porosity (ϕ) ranges from 3% to 12%. The pore volume from Archimedes principle was compared with that determined by Boyle's Law on a subset of samples, and the results showed good agreement.

Drainage cycle started after the Archimedes measurement. The toluene inside the pore space was allowed to evaporate to achieve certain target saturation (S_w). The core was subsequently enclosed in a glass bottle for fluid redistribution and thermal equilibrium. Following this, the core was weighed and loaded in the core holder. A pressure falloff measurement was performed on the core to obtain gas effective permeability (k_{eg}) at S_w . After the measurement, the core was unloaded and weighed to obtain the average saturation after gas flow. Toluene in the core was then further evaporated to achieve the next target saturation, and the falloff measurement was repeated. When k_{eg} was measured at the lowest target saturation, the imbibition cycle was started immediately by re-saturating the core with toluene to target saturations. Target saturations were chosen based on the field production information, with the lowest one close to the irreducible water saturation (S_{wirr}) in the field. Gas effective permeability (k_{eg}) at S_w was normalized to the absolute permeability (k_{abs}) to obtain relative permeability k_{rg} : $k_{rg} = k_{eg} / k_{abs}$.

RESULTS AND UNCERTAINTIES

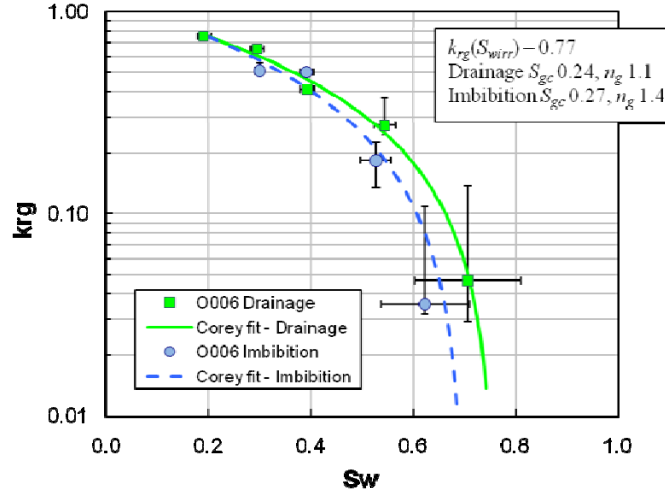


Figure 3: Drainage and imbibition gas relative permeability curves for O006.

Using the toluene/air falloff method, drainage and imbibition gas relative permeability (k_{rg}) curves have been measured on 30 tight gas core samples. An example of measured k_{rg} curves on O006 for both drainage and imbibition cycles are shown in Figure 3, where symbols are the experimental data and lines are fittings from the following Corey model:

$$k = k_{rg}(S_{wirr}) \left(\frac{1 - S_w - S_{gc}}{1 - S_{wirr} - S_{gc}} \right)^{n_g} \quad (2)$$

In Eq. (2), $k_{rg}(S_{wirr})$ is the end-point gas relative permeability at the irreducible water saturation (S_{wirr}), S_{gc} is the critical gas saturation for drainage cycle, and residual gas saturation for imbibition cycle, and n_g is the gas Corey exponent. In Figure 3 error bars are also included to illustrate the uncertainties from the measurement, and will be discussed later.

Some of measured k_{rg} data is shown in Figure 4 for Wyoming cores and Figure 5 for The North Sea cores, for drainage (a) and imbibition (b) cycles. In both figures, symbols are experimental data on individual sample grouped by the absolute permeability (k_{abs}). Dashed lines show the Corey model fitting on 3 plugs with $k_{abs} = 0.02$ mD, 0.006 mD, and 0.001 mD, respectively. Thick solid lines are two envelopes to show the general high and low boundaries to the relative permeability data. Experimentally, we mapped out a set of gas Corey parameters for those boundary cases (Table 1).

Variations in measured gas relative permeability (k_{rg}) data were observed among cores from Wyoming and those from the North Sea in Figure 4 and Figure 5, as well as in Table 1. The variations were most likely caused by cores themselves, as all the Wyoming cores were from the same field, and those North Sea cores were from two fields with different

reservoir properties. Nonetheless, some common trends were still observed. First of all, the k_{rg} curve for tight gas cores can still be described reasonably by a Corey model. End point relative permeability, $k_{rg}(S_{wirr})$, was medium to high except for two samples. Gas Corey exponent was roughly 2 for drainage cycle, and 3 for imbibition cycle. Critical gas saturation, S_{gc} , was generally higher and had large variations.

Table 1: Gas Corey Parameters for High and Low Cases in Figure 4 and Figure 5

Region	Case	$k_{rg}(S_{wirr})$	Drainage		Imbibition	
			S_{gc}	n_g	S_{gc}	n_g
Wyoming	High	0.88	0.15	1.8	0.12	2.9
	Low	0.60	0.32	1.8	0.35	2.5
North Sea	High	1.00	0.18	1.5	0.25	1.8
	Low	0.33	0.20	2.5	0.30	3.0

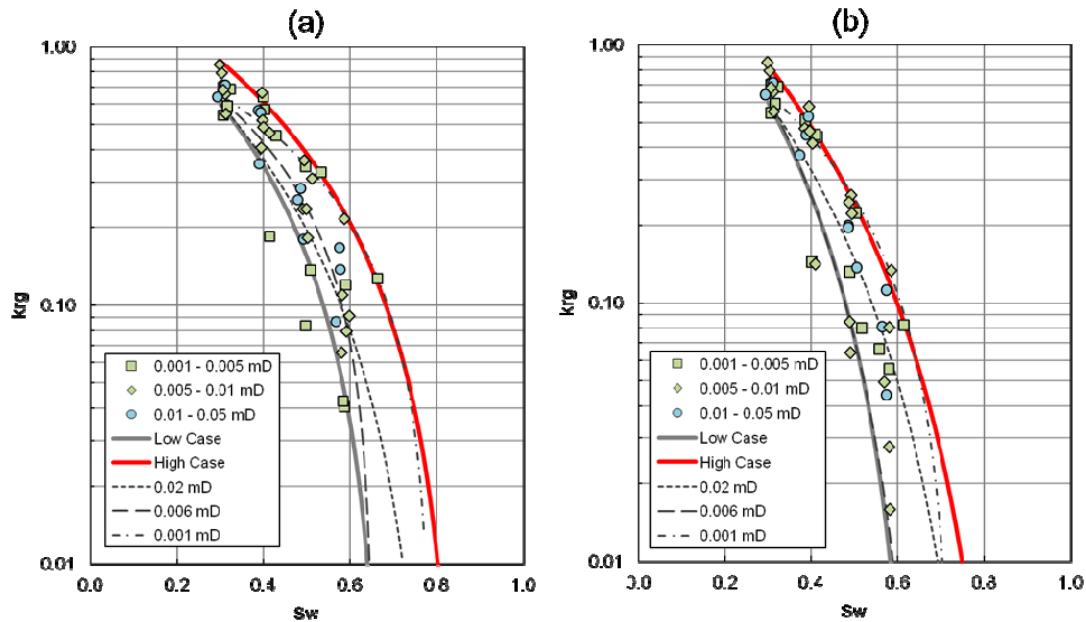


Figure 4: Gas relative permeability curves on Wyoming cores for (a) drainage cycle, and (b) imbibition cycle. See text for explanation.

To evaluate the uncertainty in Corey parameters, we first discuss the uncertainty in individual pressure falloff measurement at a certain saturation using data in Figure 3 as an example. The uncertainty in toluene saturation (S_w) was estimated from the mass difference pre- and post-falloff measurement. It was the maximum uncertainty in average toluene saturation across the whole core plug. Saturation distribution inside a core was not monitored, though. The impact of non-uniform fluid distribution on k_{rg} was studied numerically and will be discussed later.

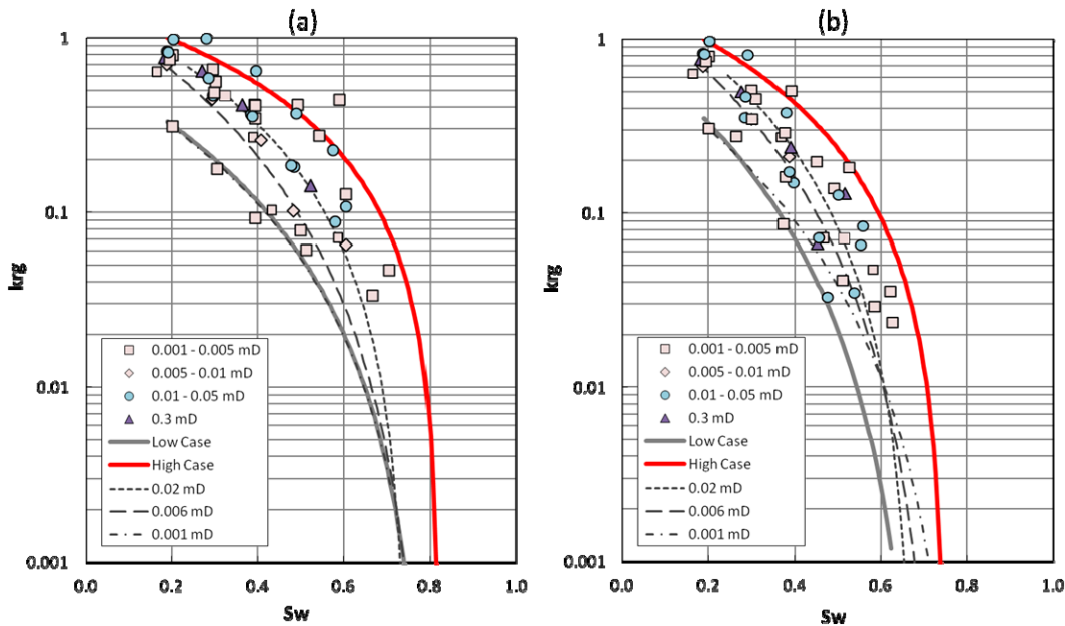


Figure 5: Gas relative permeability curves on The North Sea cores for (a) drainage cycle, and (b) imbibition cycle. See text for explanation.

The uncertainty in k_{rg} was estimated from data analysis. It represented variations in the gas effective permeability (k_{eg}) calculated from the upstream pressure decay $P_0(t)$ measured at different time during gas flow. Any effect that influences $P_0(t)$ may potentially cause uncertainty in the calculated k_{eg} . Among those effects, gas/liquid two-phase flow had the main impact. For single phase flow, calculated k_{eg} is the same no matter when the upstream pressure decay is measured as long as the assumption of constant mass flow is valid. In this method, liquid is assumed immobile during gas flow. In Figure 3, this assumption appeared to be held for $S_w < 0.5$, where k_{eg} remained the same during the entire falloff measurement. As S_w increased, liquid fractional flow started contributing to the measure pressure drop and k_{eg} varied at different time during the measurement. Consequently, the uncertainty in k_{rg} also increased. When $S_w > 0.6$, the liquid fractional flow appeared to become significant, and k_{eg} calculated from a single phase equation has large uncertainty. Another cause of variation in the measured $P_0(t)$ was from the room temperature fluctuations. In a falloff measurement on a very low permeability core, pressure decays so slow that the experiment can easily take a few hours. Moreover, k_{eg} decreases as the toluene saturation increases. Consequently, the measurement duration increases, the measured pressure decay may potentially affected by the fluctuation of room temperature. As an example of the impact from temperature variation, Figure 2 demonstrates that the uncertainty in measured permeability from falloff increases as $k < 0.001$ mD. In addition, noise from pressure transducers and microscopic heterogeneity could also affect the upstream pressure measurements and introduce uncertainties in k_{eg} .

With the above uncertainties discussion in both water saturation and relative permeability, the uncertainties in Corey parameters can be roughly estimated. End point gas relative permeability ($k_{rg}(S_{wirr})$) only depends on the permeability measurement at S_{wirr} . Critical gas saturation (S_{gc}) is largely affected by k_{rg} at higher water saturation. Gas Corey exponent (n_g) is determined from the whole curve. At low liquid saturation, the uncertainties in S_w and k_{rg} are generally small. Therefore $k_{rg}(S_{wirr})$ had less uncertainty. On the other hand, S_{gc} may have larger uncertainty because of the large uncertainties in S_w and k_{rg} at high S_w . From experimental data, uncertainty in S_{gc} varies from ± 0.05 for a core with $k_{abs} \sim 0.01$ mD to ± 0.10 for a core with $k_{abs} \sim 0.001$ mD.

NUMERICAL SIMULATION

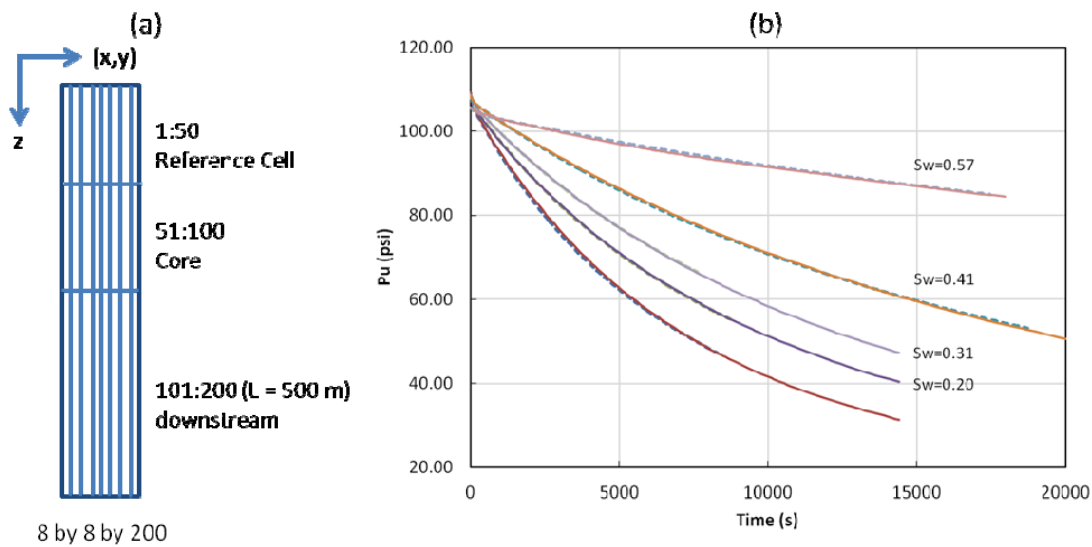


Figure 6: (a) Grid for USS gas flow simulation. (b) Pressure history matching on O006 at different S_w , where dash lines are experimental data, and solid lines are simulation results.

Table 2: Corey parameters for O006, N4, and N3

Sample	kabs (mD)	Corey Parameters From Simulation						From Exp	
		krw(Sgc)	nl	Swirr	krg(Swirr)	Sgc	ng	Sgc	ng
O006	0.004	0.1	3.5	0.19	0.77	0.39	1.0	0.24	1.1
N4	0.004	0.1	2.5	0.19	0.76	0.36	1.3	0.23	2.0
N3	0.014	0.2	4.0	0.20	1.00	0.32	1.1	0.24	1.2

Numerical simulations were performed to improve the analysis of the falloff experiment. The objectives were to study the potential impact of two-phase flow, saturation distribution and capillary pressure on upstream pressures and to evaluate Corey parameters obtained from the experiment. As shown in Figure 6(a), a 3D numerical model was built using a Shell in-house reservoir simulator. The number of grid blocks was $8 \times 8 \times 200$ in the x, y and z directions, respectively. Sizes of the grid blocks in x and

y direction were chosen such that the area in x-y plane was equal to the cross-sectional area of the core ($\sim 5 \text{ cm}^2$). In the z direction, sizes of the grid blocks were varied accordingly to honor sizes of the reference cell and the core sample. Downstream grid blocks were large enough (500 m) to maintain a constant pressure boundary.

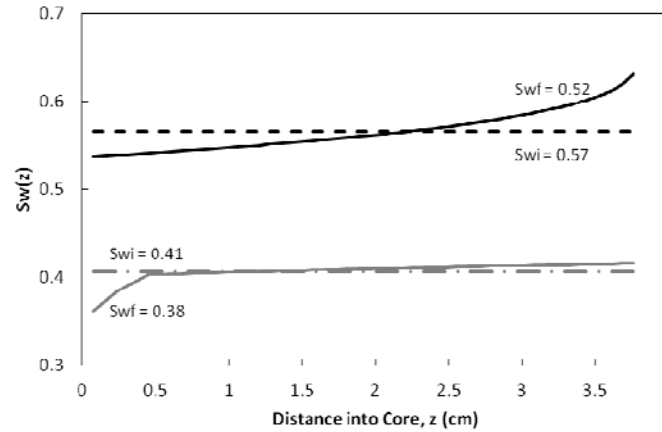


Figure 7: Saturation profiles across O006 before and after the gas flow at $S_{wi} = 0.41$ and 0.57 .

Inputs to the numerical model included the absolute permeability (k_{abs}), gas slip factor (b), Corey parameters for relative permeability curves, capillary pressure (P_c) curve, as well as fluids density and PVT properties. Among those inputs, k_{abs} and gas Corey parameters were initially from falloff measurements. Choice of b and its impact will be discussed below. There were no direct measurements available to determine the capillary pressure and liquid relative permeability. Liquid Corey parameters were chosen to represent typical water wet reservoirs, and were slightly different for different samples. The P_c curve was defined based on the stressed mercury P_c curve on a tight gas core of the similar absolute permeability. In addition, a N_2 /brine P_c curve on one of those North Sea cores with slightly higher permeability was also used as a reference. Both mercury P_c curve and N_2 /brine P_c curve were converted for the N_2 /toluene system, with the corresponding interfacial tension and contact angles.

Preliminary sensitivity study was performed on the upstream pressure decay $P_0(t)$ by varying the following inputs: initial saturation distribution $S_{wi}(x,y)$, Corey parameters, P_c , k_{abs} , and b factor. It was found that $P_0(t)$ was greatly affected by k_{abs} , b , and S_{gc} , and was much less sensitive to the change in liquid Corey parameters, $S_{wi}(x,y)$ and P_c . Based on the sensitivity study, preliminary history matching of $P_0(t)$ at different S_{wi} were performed on 3 cores. Corresponding Corey parameters are listed in Table 2. Figure 6(b) compares the simulation results of O006 at $S_{wi} = 0, 0.20, 0.31, 0.41, \text{ and } 0.57$ with the experimental data. In the simulation, the core was initialized with a uniform toluene distribution before gas flow started. And S_{gc} and n_g were adjusted to match $P_0(t)$. Overall good agreement was observed from Figure 6. For the Gas Corey parameters obtained from history matching, n_g agreed well with that from the experiment, while S_{gc} was higher.

Liquid saturation profiles across the core before and after the gas flow are shown in Figure 7 for O006 at $S_{wi} = 0.41$ and 0.57 . Where dash lines represent the initial saturation profiles and the solid lines are the final profiles after gas flow. Liquid saturation can be considered as uniform approximately for most portion of the core. For $S_{wi} = 0.41$, first 5 mm of the core was drier, probably due to the gas flow at the beginning of falloff measurement when the flow rate was the highest. At $S_{wi} = 0.57$, capillary end effect caused the saturation gradient close to the downstream side. Simulation suggested that for lower P_c , capillary end effect gets worse and the saturation gradient inside the core increases. In current work, only $P_0(t)$ is measured directly and used in history matching. The determination of gas Corey parameters is not sensitive to the variation in P_c curve. Additional imaging technique may shed insight on it.

Note that in the above history matching, S_{gc} and n_g were adjusted while k_{abs} and b were fixed. From the sensitivity study, b affected $P_0(t)$ greatly too. Sampath et al. studied the effect of saturation on b and correlated b to k_{abs} and ϕ [4]. However, the pore pressures used in their permeability measurements were relatively low and varied in a small range (between 20 psi to 35 psi). It may cause large uncertainties during the extrapolation to obtain b . In this work, we measured both Klinkenberg permeability and b factor on O006 using SPPOP at $S_w = 0.2$, where the liquid was immobile. The result indicated a decrease in b : $b = 102$ psi at $S_w = 0.2$ as compared with $b = 141$ psi on the dry core. While further study on the relation between b and S_w is needed and currently ongoing, for simulations in this work, b was adjusted to match $P_0(t)$ at S_{wirr} for each sample, and then fixed for other runs at other S_w . As S_{gc} and b affect $P_0(t)$ in the opposite direction, ie. $P_0(t)$ decreased as S_{gc} increases or b decreases. S_{gc} from simulation with b value fixed may be higher than a true case.

DISCUSSION

In the gas relative permeability measurement, we have made assumptions of immobile and uniform distributed liquid phase during gas flow in a tight pore system. Determining under what circumstance those assumptions hold is the key to the application of this method. Our analysis has shown that gas flow in a tight gas core with partial liquid saturation can be treated as single phase flow for $S_w \leq 0.5$, because liquid is immobile and does not change the distribution during gas flow. As $S_w \geq 0.6$, liquid starts flowing and saturation gradient develops along gas flow direction due to the capillary end effect. k_{eg} from $P_0(t)$ using single phase formula may have large uncertainties.

In this section, we further discuss initial fluid distribution and its potential impact on relative permeability measurement with the aid of simulation study. Liquid saturation in the core is varied by evaporation. While this method is relatively easy and quick, a non-uniform saturation distribution inside the core by evaporation is of prime concern. The saturation gradient is established during evaporation as the outside portion of the core dries out first. Experimentally, this gradient is mitigated by enclosing the core with certain target saturation in a glass bottle for an extended period of time. Previous study

showed that this method can effectively redistribute the fluid more uniformly [10]. In this work, we also evaluated the timing for equilibrium by a series of toluene/air counter-current imbibition measurements. Our measurements showed that it typically takes 15 to 30 minutes to achieve capillary equilibrium (end of spontaneous imbibition) for a tight core with certain initial gas saturation.

While the core is enclosed in the bottle, fluid imbibes from inside spontaneously. As a result, the inside portion of core is further drained, and the outer portion undergoes an imbibition process. From this point of view, drainage k_{rg} measured by the evaporation method is probably not a true drainage k_{rg} curve, but a “mixed” curve. Chowdiah [11, 12] argued that k_{rg} from evaporation was lower than that from a true drainage type experiment due to pore throat blockage by imbibition. However, other experiments showed that results from evaporation did not differ immediately from those from centrifuge or porous plate [1]. The counter-current imbibition measurements also showed that for most of the tight gas cores in this work, the residual gas saturation due to capillary trapping was around 0.2 – 0.3, less than that in a Berea sandstone (~ 0.4).

The drainage and imbibition processes stop when the entire core reaches the capillary equilibrium. As the capillary pressure changes in the outer portion of the core along the imbibition cycle, the fluid saturation might be slightly lower than that for the inside of the core at the same capillary pressure. In other words, small saturation gradients may exist in the plane perpendicular to the gas flow $S_{wi}(x,y)$. However, numerical studies suggest that its impact on the upstream pressure can be ignored, thus does not affect the Corey parameters.

CONCLUSION

We have applied a toluene/air pressure falloff method to characterize the gas phase relative permeability for tight gas cores. Toluene is used as the wetting phase and varied by evaporation. Its distribution is approximately uniform through a combination of drainage and imbibition process inside the core. Gas effective permeability is measured by pressure falloff method, and the gas relative permeability curve is described by a Corey model. Numerical simulations confirm that for $S_w < 0.5$ the liquid is immobile during gas flow and capillary pressure does not affect the pressure decay. At $S_w \geq 0.6$, saturation gradient along the core develops due to the mobile liquid and capillary end effect. As for Gas Corey parameters, both the falloff measurement and simulations agree reasonably on Corey exponent n_g , and show large uncertainty in critical gas saturation S_{gc} .

The toluene/air falloff method simplifies the experimental setup and greatly reduces the measurement duration. It has been proven to be an effective way to measure gas relative permeability and provided important input to dynamic reservoir modeling. We have applied the method in gas relative permeability measurements on 30 core samples from

both USA and the North Sea. Results show a Corey exponent of ~ 2 for drainage cycle and ~ 3 for imbibition cycle.

ACKNOWLEDGEMENTS

We thank Peter Doe for insightful discussions, Steve Shi and Ralf Hedden for generous help on numerical modeling, and Richard Rosen and Peter Zannitto for their initial valuable contribution to the method development.

REFERENCES

1. A. P. Byrnes, "Issues with gas relative permeability in low-permeability sandstones", in *Understanding, exploring, and developing tight-gas sands - 2003 Vail Hedberg Conference*, S. P. Cumella, K. W. Shanley, and W. Camp (Editors), American Association of Petroleum Geologists Hedberg Series, no. 3, Chapter 5 (2008).
2. R. M. Cluff and A. P. Byrnes, "Relative permeability in tight gas sandstone reservoirs - The 'Permeability Jail' Model", *SPWLA 51st Annual Logging Symposium* (2010).
3. R. D. Thomas and D. C. Ward, "Effect of overburden pressure and water saturation on gas permeability of tight sandstone cores", *SPE* 3634-PA (1972).
4. K. Sampath and C. William Keighin, "Factors affecting gas slippage in tight sandstones of cretaceous age in the Uinta Basin", *SPE* 9872 (1981).
5. J. D. Walls, A. M. Nur, and T. Bourbie, "Effects of pressure and partial water saturation on gas permeability in tight sands: experimental result", *SPE* 9378-PA (1982).
6. J. S. Ward and N. R. Morrow, "Capillary pressure and gas relative permeability of low permeability sandstone", *SPE* 13882-PA (1987).
7. S. C. Jones, "A rapid accurate unsteady-state Klinkenberg permeameter", *SPE Journal*, **12**, 383–397 (1972).
8. J. A. Rushing, K. E. Newsham, P. M. Lasswell, J. C. Cox, and T. A. Blasingame, "Klinkenberg-corrected permeability measurements in tight gas sands: steady-state versus unsteady-state technique", *SPE* 89867 (2004).
9. Y. Wang and R. J. Knabe, "Permeability characterization on tight gas samples using pore pressure oscillation method", *SCA Proceeding* 2010-30.
10. J. J. Pickell, B. F. Swanson, and W. B. Hickman, "Application of air-mercury and oil-air capillary pressure data in the study of pore structure and fluid distribution", *SPE* 1227-PA.
11. P. Chowdiah, "Laboratory measurements relevant to two-phase flow in a tight gas sand matrix", *SPE* 16945 (1987).
12. P. Chowdiah, "Influence of water-desaturation technique and stress on laboratory measurement of hydraulic properties of tight sandstones", *SPE* 15210 (1988).